

© 2022. This manuscript version is made available under the CC-BY-NC-ND 4.0 license: <http://creativecommons.org/licenses/by-nc-nd/4.0/>

Cucurbit[6]uril-Based Supramolecular Frameworks formed through Outer Surface Interactions and Application for Iodine Adsorption

Jian-Hang Hu ^a, Ran Cen ^a, Ming Liu ^a, Pei-Hui Shan ^a, Timothy J. Prior,^b Carl Redshaw ^b, Ying Huang ^a, Zhu Tao ^a, Xin Xiao ^{a,*}

^a Key Laboratory of Macrocyclic and Supramolecular Chemistry of Guizhou Province, Institute of Applied Chemistry, Guizhou University, Guiyang 550025, China.

^b Department of Chemistry, University of Hull, Hull HU6 7RX, U.K.

Abstract: The interaction between the outer surface of cucurbit[6]uril (Q[6]) and methyl triphenyl phosphorus iodide (MTPI) has been studied in the presence of $[\text{CdCl}_4]^{2-}$. The MTPI is connected to four neighboring Q[6]s through weak interactions such as $\text{C-H}\cdots\pi$ and $\text{C-H}\cdots\text{O}$, whilst the $[\text{CdCl}_4]^{2-}$ is connected with the portal carbonyl oxygen, glycoside urea methylene and a bridging methylene of a Q[6] molecule via ion-dipole interactions. These interactions were evident from a single crystal X-ray diffraction study of $\text{Q[6]-MTPI-}[\text{CdCl}_4]_2$. Furthermore, this complex exhibits a porous structure, which can be described as a Q[6]-based supramolecular framework (QSF), and its ability to adsorb iodine was also investigated.

Keywords: Cucurbit[6]uril; methyl triphenyl phosphorus iodide; weak interactions; Q[n]-based supramolecular framework; outer surface interactions.

Introduction

In recent years, supramolecular self-assembly has attracted extensive attention due

to its applications in many research fields such as chemistry, materials, environmental and life science [1-7]. Selecting different building blocks and constructing supramolecular self-assembly systems with novel structures and various properties through weak interactions such as intermolecular hydrogen bonds and ion-ion dipoles has become an important method for constructing new systems.

Cucurbit[*n*]urils (Q[*n*]s) [8], as a kind of macrocyclic compound, are being increasingly used for the construction of supramolecular assemblies. They possess a near electrically neutral cavity, two negatively charged carbonyl oxygen portals, and a positively charged outer surface (figure 1). It is precisely because of these structural characteristics that Q[*n*]s are seeing increased usage in supramolecular chemistry, with progress reported in Q[*n*]s host-guest chemistry [9-14] and Q[*n*]s coordination chemistry [15-17].

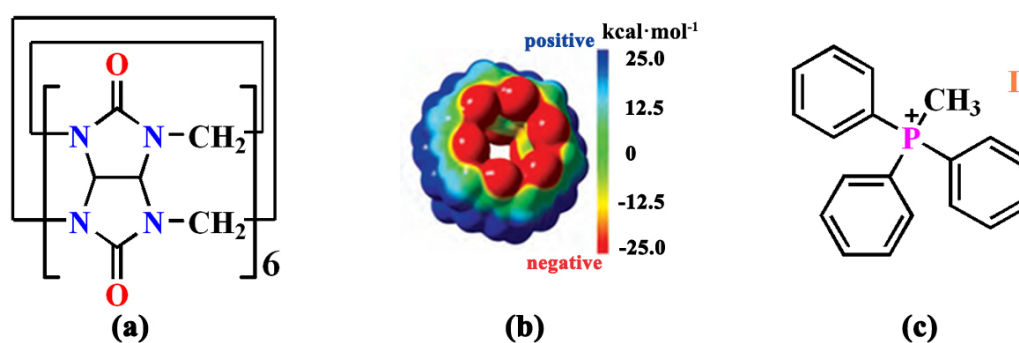


Figure 1. (a) Structural diagram of Q[6]; (b) surface electrostatic potential diagram of Q[6]; (c) structure of methyl triphenyl phosphorus iodide.

Our laboratory and others have been working on Q[*n*]-based supramolecular frameworks based on OSIQs since 2014 [18-24], when we first proposed the outer surface interactions of Q[*n*]s (OSIQ) [18], specifically self and anion-induced OSIQs [19], which involved the electrostatic potential positive outer surface of Q[*n*]s. Further research has showed that Q[*n*]-based coordination polymers and frameworks can be utilized to recover a wide range of metal ions [23,24], as well as to prepare various sensors [25-31].

Over the last ten years, there has been a trend of constructing supramolecular

organic frameworks with structural characteristics based on weak intermolecular interactions, including hydrogen bonds, ion–dipole interactions, C-H $\cdots\pi$ interactions, and $\pi\cdots\pi$ interactions [32]. Since the driving force originates from supramolecular interactions, supramolecular organic frameworks (SOFs) are usually easy to synthesize and exhibit good reversibility. On the other hand, SOFs usually lack sufficient strength and stability. Therefore, choosing organic building blocks with rigid structures to construct SOFs may be an effective path to overcome these drawbacks [32,33]. In fact, there is a simpler and more efficient way to construct Q[*n*]-based supramolecular framework (QSF) through the action of outer the surface [18]. The driving force originates from the positive electrostatic potential of the Q[*n*] at the outer surface. The QSF assembly process can be loosely split into three types based on the different species interacting with the outer surface of Q[*n*]: self-induced, anion-induced, and aromatic-ring-induced (termed aromatic-induced hereafter).

MTPI can be used as a Wittig reagent. In 1953, the German scientist G. Wittig discovered diphenyl ketone reacted with methylene triphenyl phosphorane to afford vinylidene in high yield. This reaction has attracted the attention of organic chemists and it is now known as the Wittig reaction [34,35]. It has been widely used in the synthesis of various green herbicidal and herbicidal pesticides, insect pheromones, new pharmaceuticals and their intermediates, ethane liquid crystals, organic luminescent materials, important antibiotics, light conductors and for other advanced fine organic chemicals of different kinds [36,37]. In addition, methyl triphenyl phosphorus iodide is a reactant in the synthesis of triphenyl dyes and aromatic molecules of polyolefins [38]. Interestingly, the molecular structure of MTPI has three aromatic rings with different spatial directions which can serve as C-H $\cdots\pi$, $\pi\cdots\pi$ interaction sites, and this contributes to the formation of cucurbit[*n*]uril-based supramolecular self-assemblies. Here, we report a new QSF material which is converted into the Q[6]-MTPI-[CdCl₄]₂ supramolecular framework material on introduction of MTPI and [CdCl₄]²⁻ to Q[6] in acidic solution. A description of its structure, characteristics, and use for the adsorption of I₂ is discussed.

Experimental section

Materials

MTPI was purchased from Aladdin (Shanghai, China) and used as supplied without further purification. Q[6] was prepared according to a literature method [39].

Single-crystal X-ray crystallography

The crystal structure of Q[6]-MTPI-[CdCl₄]²⁻ was determined using data collected using a Bruker D8 venture single crystal diffractometer. The single crystal of the complex was grown from 6M HCl solution by solvent evaporation. A graphite monochromator, Mo K α radiation source ($\lambda = 0.71073 \text{ \AA}$, $L=0.828 \text{ mm}^{-1}$), temperature (293K) and a ω -Scan mode were employed. The SAINT program was used to correct the data for the Lorentz effect and polarization effect, and SADABS was used to apply a semi empirical absorption correction based on equivalent reflections. The structure was solved by dual space methods in SHELXT and the structure refined using SHELXL-2018^[40,41] implemented within Olex2^[42]. All non-hydrogen atoms of the main molecules were refined using anisotropic displacement parameters. Carbon bound hydrogen atoms were introduced into the calculation position and regarded as riding atoms. Their isotropic displacement parameters are equal to 1.2 times of the parent atom. Table 1 summarizes the details of crystal parameters, data collection conditions and refinement statistics, and the crystal data have been deposited in the Cambridge crystal data center as a supplementary publication (CCDC-2161688). These data can be obtained free of charge via http://www.ccdc.cam.ac.uk/data_request/cif, by emailing data_request@ccdc.cam.ac.uk, or by contacting The Cambridge Crystallographic Data Centre, 12, Union Road, Cambridge CB21EZ, UK (fax: +44 1223 336033).

Preparation of complex Q[6]-MTPI-[CdCl₄]₂

To a solution of MTPI (10 mg, 0.025 mmol) in 3 ml of 6M HCl, Q[6] (10 mg,

0.010 mmol) was added, then $\text{CdCl}_2 \cdot 2.5 \text{H}_2\text{O}$ (10 mg, 0.044 mmol) was also added to this solution. The mixture was heated until it is completely dissolved. The filtrate was evaporated slowly under air for about two weeks, and diamond red crystals of compound $\text{Q}[6]\text{-MTPI-}[\text{CdCl}_4]_2$ were obtained in a yield of 2.9 mg (20%).

Results and discussion

Cucurbit[6]uril-based supramolecular frameworks structures

Given that a $\text{Q}[n]$ possesses outer surface interactions with positive electrostatic potential, various kinds of $\text{Q}[n]$ -based supramolecular framework materials with different structural features can be constructed through its outer surface. The ways in which QSFs can form can be classified as: self-induced, induced by inorganic anions, and induced by organic aromatic compounds. Various QSFs are formed by organic aromatics that interact with the positive electrostatic potential OSIQ via hydrogen bonding, $\text{C-H}\cdots\pi$, $\text{C-H}\cdots\text{O}$, and ion-ion dipole interactions. Herein, we report the synthesis of a $\text{Q}[6]$ -based QSF with methyl triphenyl phosphorus iodide (MTPI) as a structure directing agent to obtain a three-dimensional structure. We have focused on $\text{Q}[6]$ -aromatic organic compounds-inorganic anion induced QSFs. Following the preparation outlined in the experimental section, red crystals were obtained. The crystal structure is shown in figure 2a and all measured distances are based on the interaction between hydrogen atoms and receptors. The crystal data shows that Cl^- on the $[\text{CdCl}_4]^{2-}$ anion forms an ion dipole interaction with the carbonyl carbon of $\text{Q}[6]$ while also forming an $\text{C-H}\cdots\text{Cl}^-$ interaction with aromatic rings on MTPI with bond lengths of 3.379 Å and 2.893 Å, respectively (figure 2b). To facilitate visualization we omitted $[\text{CdCl}_4]^{2-}$, and one can see the action of the two MTPI molecules with the same $\text{Q}[6]$ molecule (figure 2c). This agrees with the QSFs induced by our aromatic organic compounds described above. The bond lengths for the left MTPI interacting with the $\text{Q}[6]$ port carbonyl oxygen from top to bottom are 2.445 Å, 2.783 Å and 2.757 Å, while for the right MTPI interacting with $\text{Q}[6]$, there are two modes of $\text{C-H}\cdots\pi$ interacting with $\text{C-H}\cdots\text{O}$ at bond lengths of 2.802 Å, 2.753 Å and 2.586 Å respectively.

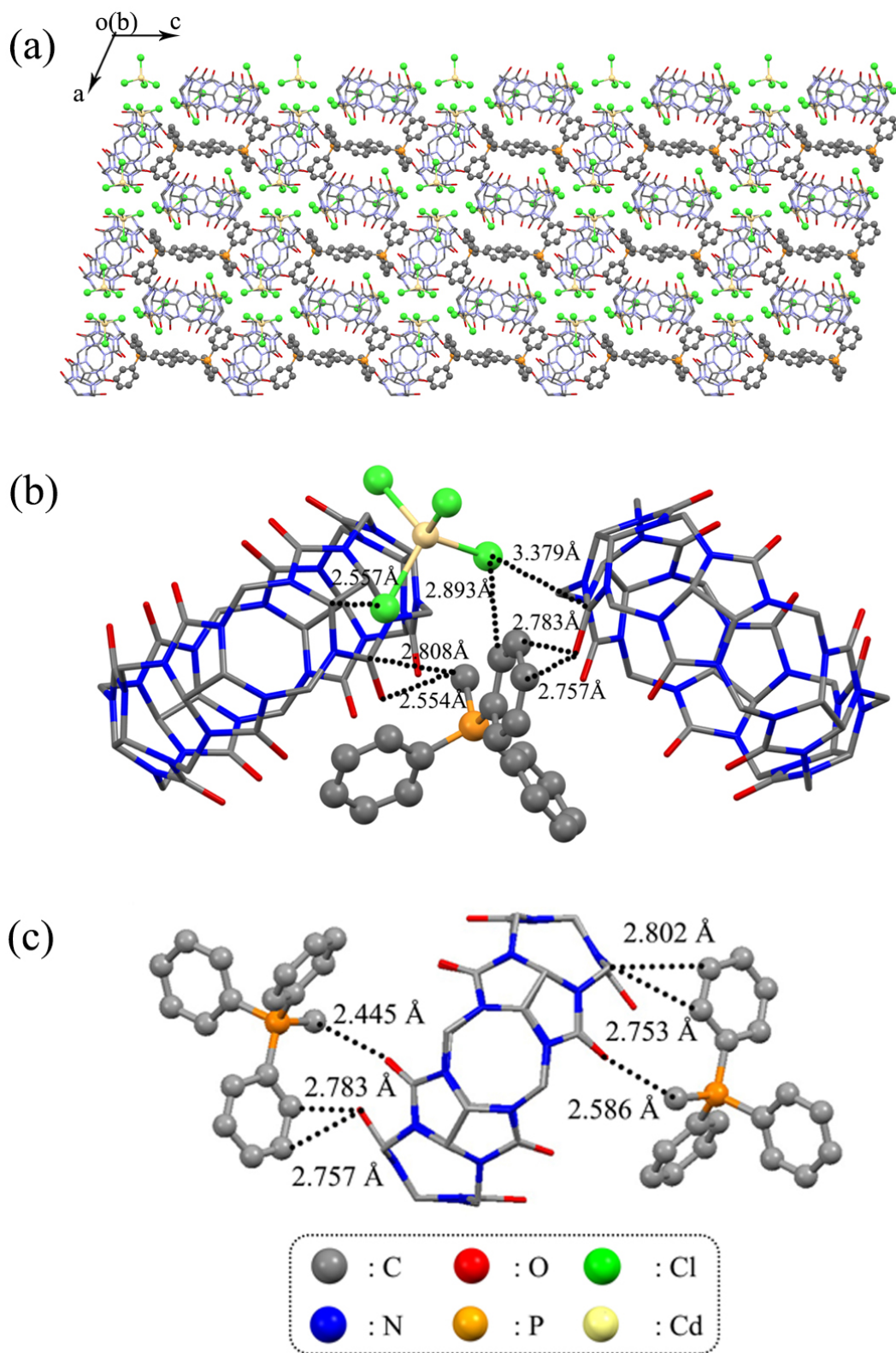


Figure 2. Three-dimensional view of the crystal structure of Q[6]-MTPI-[CdCl₄]²⁻.

Now, we will describe Q[*n*]-based the supramolecular framework structure from a

more specific perspective. Figure 3a displays the basic building block of a Q[6]-based QSF constructed by the interaction of four Q[6] molecules with MTPI. Various interactions within the unit structure include the interactions between MTPI and Q[6]s, and the interactions between Q[6]s only. More specifically, interactions include: I) the formation of C-H \cdots O interactions between the methyl group of MTPI and the first Q[6] portal carbonyl oxygen, and C-H \cdots π interactions between the aromatic ring of MTPI and the bridging methylene group of Q[6] (figure 3b); II) the C-H \cdots O interactions between the C-H on the aromatic ring of MTPI and the second Q[6] portal carbonyl oxygen, and C-H \cdots π interactions between the aglycone methine of Q[6] and MTPI (figure 3c); III) the C-H \cdots π interactions formed between the other aromatic ring of MTPI and the aglycone methine of Q[6], and C-H \cdots O interactions formed between the same aromatic ring and the third Q[6] portal carbonyl oxygen (figure 3d); IV) the methyl group of MTPI also forms a C-H \cdots O interaction with the fourth Q[6] portal carbonyl oxygen (figure 3e). We note that Q[6] oxygen...OH₂ distances for closest approach are around 2.70 to 2.95 Å. Additionally, there is no evidence for the protonation of the Q[6] molecules; the C=O distances have mean value 1.228 Å with standard deviation 0.007 Å and there are no outliers.

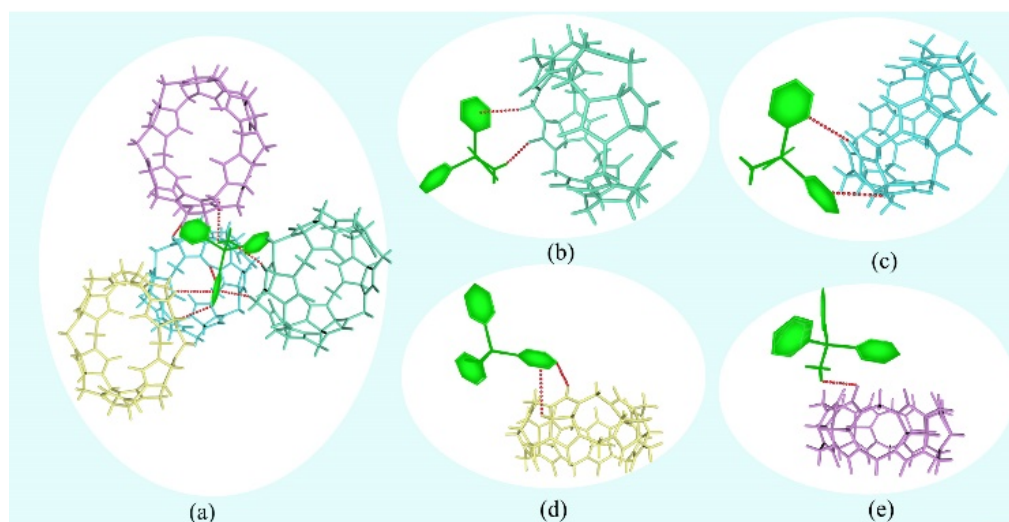


Figure 3. Q[6]-MTPI outer surface interactions.

The positive electrostatic potential outer surface interactions of Q[*n*] can occur not

only with adjacent aromatic organic compounds but also with negatively charged species (especially anions). Under suitable conditions, Q[*n*] molecules and anions readily form QSFs. For example, when transition metal ions are introduced into the Q[*n*]-MTPI system, it easily forms polychlorinated transition metal anions. As shown in figure 4a, [CdCl₄]²⁻ can be connected by ion dipole interactions between the portal carbonyl carbon of the Q[6] molecule, the aglycone methine as well as the bridging methylene groups. In addition to the above two kinds of outer surface Q[*n*] interactions, the Q[*n*]s portal carbonyl oxygen can interact with the positive electrostatic potential outer wall of adjacent Q[*n*]s through dipole interactions to form various QSFs. These effects include the portal carbonyl oxygen atom of a Q[*n*] molecule with the methine unit of an adjacent Q[*n*], a bridging methylene unit, and dipole interactions between the portal carbonyl carbon atoms (figure 4b).

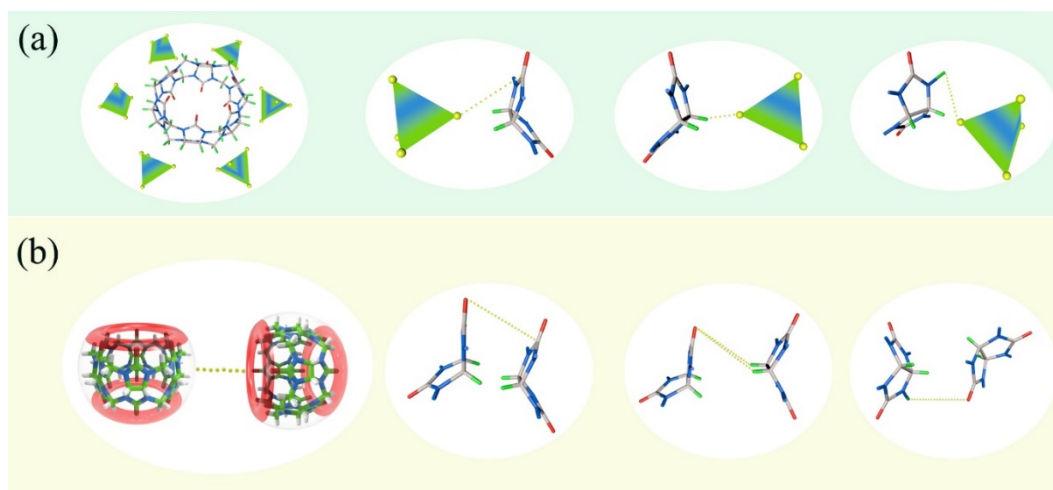


Figure 4. (a) The Q[6]-[CdCl₄]²⁻ interactions; (b) Self-induced Q[6]-Q[6].

Sorption properties of iodine

In order to explore the iodine adsorption performance of this Q[*n*]-based supramolecular framework material, it was necessary to draw the standard curve of iodine (Figure 5), and use the standard curve to find the appropriate adsorbed concentration of iodine solution. We then measured the UV absorption value of the corresponding solution according to the adsorption concentration of the fixed iodine

solution and different adsorption time intervals, and calculated the adsorption efficiency and adsorption capacity of iodine according to the UV absorption value.

The adsorption efficiency is calculated by the following formula to obtain the adsorption of iodine by adsorbent Q[6]-MTPI [43].

$$\% \text{Pollutant removal efficiency} = ((C_0 - C_t) / C_0) \times 100\%$$

where C_0 represents the initial concentration of pollutants and C_t represents the concentration of pollutants in the filtrate after adsorption.

The load of adsorbent on pollutants is calculated by the following formula [44].

$$Q_t = (C_0 - C_t) V / m$$

where C_0 and C_t (mg/L) are the initial and equilibrium concentrations, respectively, of the iodine solution; V (L) is the volume of the solution; and m (g) is the weight of Q[6]-MTPI-[CdCl₄]²⁻ crystals used.

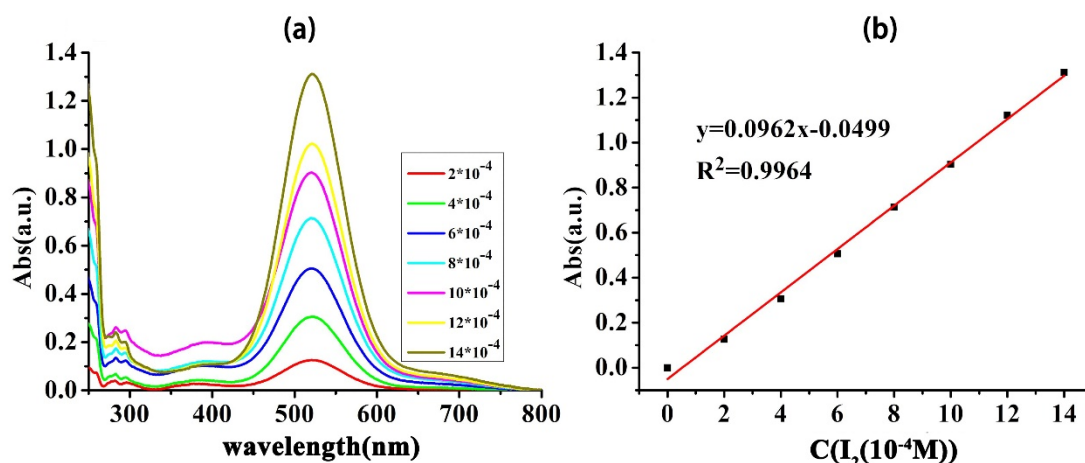


Figure 5. UV absorption diagram and standard curve of I₂ at different concentrations.

Following this, 20 mg Q[6]-MTPI-[CdCl₄]²⁻ red single crystals was weighed and immersed in 10 ml of 4 × 10⁻⁴ M iodine solution. After the addition of the single crystals, the color of the cyclohexane solution gradually fades from deep red to almost colorless. Figure 6a shows the adsorption of iodine by the single crystal samples. Through calculations, the adsorption efficiency of the adsorbent Q[6]-MTPI for I₂ was found to be 30.8% and the adsorption capacity 202.7 mg/g. As shown in figure 6b, the change

of intensity of the iodine absorption decreases linearly with time at 521 nm.

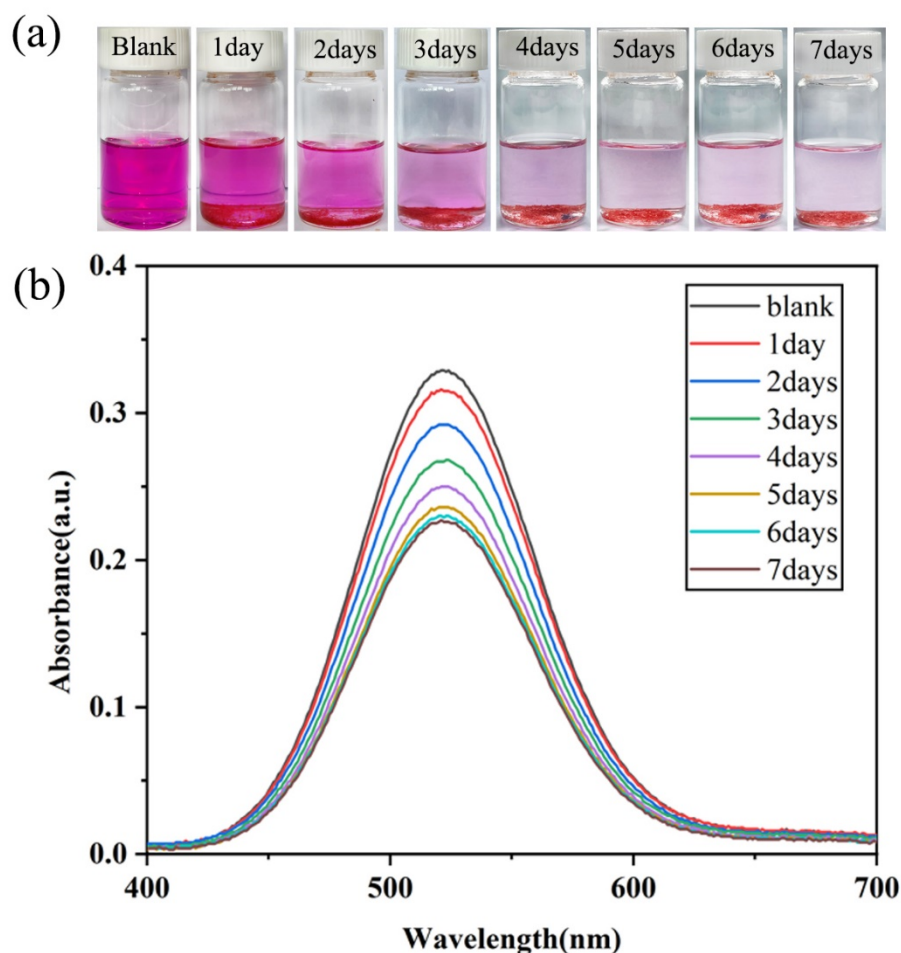


Figure 6. (a) Photo of the iodine adsorption process, in which 20 mg of red crystals is immersed in cyclohexane solution containing I_2 ; (b) Evolution of UV-Vis absorption spectra of I_2 adsorbed by single crystals in 10 ml cyclohexane solution.

Conclusion

In short, we found that the host Q[6] and the guest MTPI can form an outer surface interaction mode in acidic solution. We have characterized the system by a series of techniques such as X-ray crystallography and UV-Vis absorption spectra. Our work shows the driving force for the formation of the Q[6]-based supramolecular frameworks (Q[6]-MTPI-[CdCl₄]₂) is the weak interactions between the guest and host, such as C-H \cdots π , C-H \cdots O, and the ion-dipole interactions between the inorganic metal anions and host-guest. Furthermore, we also used the crystals as a Q[n]-based supramolecular

framework material to adsorb iodine.

Table 1. Crystal data and structure refinement for MTPI

Empirical formula	C ₅₅ H ₅₄ Cd ₂ Cl ₈ N ₂₄ O ₂₄ P
Formula weight	1974.59
Temperature/K	293.15
Crystal system	triclinic
Space group	P-1
a/Å	14.326(3)
b/Å	16.498(4)
c/Å	19.211(4)
α/°	95.883(8)
β/°	96.498(7)
γ/°	115.045(8)
Volume/Å ³	4029.9(16)
Z	2
ρ _{calc} /cm ³	1.627
μ/mm ⁻¹	0.879
F(000)	1982.0
Crystal size/mm ³	0.14 × 0.13 × 0.12
Radiation	MoKα (λ = 0.71073)
2θ range for data collection/°	4.73 to 53.83
Index ranges	-18 ≤ h ≤ 18, -21 ≤ k ≤ 21, -24 ≤ l ≤ 24
Reflections collected	171465
Independent reflections	17430 [R _{int} = 0.0827, R _{sigma} = 0.0453]
Data/restraints/parameters	17430/168/1018
Goodness-of-fit on F ²	1.026
Final R indexes [I ≥ 2σ (I)]	R ₁ = 0.0644, wR ₂ = 0.1817
Final R indexes [all data]	R ₁ = 0.0781, wR ₂ = 0.1973
Largest diff. peak/hole / e Å ⁻³	1.49/-1.24

Acknowledgments

This work was supported by the National Natural Science Foundation of China (No. 22061009) and the Innovation Program for High-level Talents of Guizhou

Province (No. 2016-5657). CR thanks the EPSRC for an Overseas Travel Grant (EP/R023816/1).

Conflict of Interest

There are no conflict of interest.

References

- [1] C. J. Kuehl, Y. K. Kryshenko, U. Radhakrishnan, S. R. Seidel, S. D. Huang, P. J. Stang. Self-assembly of nanoscopic coordination cages of D(3h) symmetry. *PNAS*, 2002, 99 (8), 4932-4936.
- [2] H. J. Kim, T. Kim, M. Lee. Responsive nanostructures from aqueous assembly of rigid-flexible block molecules. *Acc. Chem. Res.*, 2011,44 (1), 72-82.
- [3] C. Sanchez, H. Arribart, M. M. G. Guille. Biomimetism and bioinspiration as tools for the design of innovative materials and systems. *Nature Mat*, 2005, 4 (4), 277-288.
- [4] C. A. Orme, A. Noy, A. Wierzbicki, M. T. McBride, M. Grantham, H. H. Teng, P. M. Dove, J. J. DeYoreo. Formation of chiral morphologies through selective binding of amino acids to calcite surface steps. *Nature*, 2001, 411, 775-779.
- [5] W. Zhang, Y. Luo, J. Zhao, W.-H. Lin, X.-L. Ni, Z. Tao, X. Xiao, C.-D. Xiao. tQ[14]-based AIE Supramolecular Network Polymers as Potential Bioimaging Agents for the Detection of Fe³⁺ in Live HeLa Cells. *Sensors and Actuators B-Chemical*, 2022, 354, 131189.
- [6] K.-K. Yang, G.-C. Yu, Z.-Q. Yang, L.-D. Yue, X.-J. Zhang, C. Sun, J.-W. Wei, L. Rao, X.-Y. Chen, R.-B. Wang. Supramolecular Polymerization-Induced Nanoassemblies for Self-Augmented Cascade Chemotherapy and Chemodynamic Therapy of Tumor. *Angew. Chem. Int. Ed.*, 2021, 60, 17570-17578.
- [7] J. Chen, S.-K. Li, Z.-Y. Wang, Y.-T. Pan, J.-W. Wei, S.-Y. Lu, Q.-W. Zhang, L.-H. Wang, R.-B. Wang. Synthesis of an AIEgen functionalized cucurbit[7]uril for subcellular bioimaging and synergistic photodynamic therapy and supramolecular chemotherapy. *Chem. Sci.*, 2021, 12, 7727-7734.
- [8] H. Cong, X.-L. Ni, X. Xiao, Y. Huang, Q.-J. Zhu, S.-F. Xue, Z. Tao, L. F. Lindoy,

- G. Wei. Synthesis and separation of cucurbit[n]urils and their derivatives. *Org. Biomol. Chem.*, 2016, 14 (19), 4335-4364.
- [9] X. Xiao, W.-J. Li, J.-Z. Jiang. Porphyrin-cucurbituril organic molecular porous material: Structure and iodine adsorption properties. *Inorg. Chem. Commun.*, 2013, 35, 156-159.
- [10] K. Kim, N. Selvapalam, Y. H. Ko, K. M. Park, D. Kim, J. Kim. Functionalized cucurbiturils and their applications. *Chem. Soc. Rev.*, 2007, 36 (2), 267-279.
- [11] E. Masson, X.-X. Ling, R. Joseph, L. K. Mensah, X.-Y. Lu. Cucurbituril chemistry: a tale of supramolecular success. *RSC Adv.*, 2012, 2 (4), 1213-1247.
- [12] Y.-L. Liu, Z.-H. Huang, X.-X. Tan, Z.-Q. Wang, X. Zhang. Cucurbit[8]uril-based supramolecular polymers. *Chem. Asian. J.*, 2013, 8 (8), 1626-1632.
- [13] L. Isaacs. Stimuli responsive systems constructed using cucurbit[n]uril-type molecular containers. *Acc. Chem. Res.*, 2014, 47 (7), 2052-2062.
- [14] K. I. Assaf, W. M. Nau. Cucurbiturils: from synthesis to high-affinity binding and catalysis. *Chem. Soc. Rev.*, 2015, 44 (2), 394-418.
- [15] Y. Luo, W. Zhang, M. Liu, J. Zhao, Y. Fan, B. Bian, Z. Tao, X. Xiao. A supramolecular fluorescent probe based on cucurbit[10]uril for sensing the pesticide dodine. *Chinese Chem. Lett.*, 2021, 32, 367-370.
- [16] D. Yang, M. Liu, X. Xiao, Z. Tao, C. Redshaw. Polymeric self-assembled cucurbit[n]urils: Synthesis, structures and applications. *Coordin. Chem. Rev.*, 2021, 434, 213733.
- [17] X.-L. Ni, S.-F. Xue, Z. Tao, Q.-J. Zhu, L. F. Lindoy, G. Wei. Advances in the lanthanide metallosupramolecular chemistry of the cucurbit[n]urils. *Coord. Chem. Rev.*, 2015, 287, 89-113.
- [18] X.-L. Ni, X. Xiao, H. Cong, Q.-J. Zhu, S.-F. Xue, Z. Tao. Self-assemblies based on the “outer-surface interactions” of cucurbit[n]urils: new opportunities for supramolecular architectures and materials. *Acc. Chem. Res.*, 2014, 47(4), 1386-1395.
- [19] Y. Huang, R.-H. Gao, M. Liu, L.-X. Chen, X.-L. Ni, X. Xiao, H. Cong, Q.-J. Zhu, K. Chen, Z. Tao. Cucurbit[n]uril-Based Supramolecular Frameworks Assembled through Outer-Surface Interactions. *Angew. Chem. Int. Ed.*, 2021, 60 (28), 15166-15191.

- [20] I. Hwang, W. S. Jeon Dr., H.-J. Kim Dr., D. Kim Dr., H. Kim, N. Selvapalam Dr., N. Fujita Dr., S. Shinkai Prof. Dr., K. Kim Prof. Dr. Cucurbit[7]uril: A Simple Macrocyclic, pH-Hydrogelator Exhibiting Guest-Induced Stimuli-Responsive Behavior. *Angew. Chem. Int. Ed.*, 2007, 46, 210-213.
- [21] K. I. Assaf, W. M. Nau. The chaotropic effect as an assembly motif in chemistry. *Angew. Chem. Int. Ed.*, 2018, 57, 13968-13981.
- [22] X.-K. Fang, P. Kögerler, L. Isaacs, S. Uchida, N. Mizuno. Cucurbit[n]uril-Polyoxoanion Hybrids. *J. Am. Chem. Soc.*, 2009, 131, 432-433.
- [23] Y.-Q. Yao, Y.-J. Zhang, C. Huang, Q.-J. Zhu, Z. Tao, X.-L. Ni, G. Wei. Cucurbit[10]uril-based smart supramolecular organic frameworks in selective isolation of metal cations. *Chem. Mater.*, 2017, 39, 5468–5472.
- [24] L.-X. Chen, M. Liu, Y.-Q. Zhang, Q.-J. Zhu, J.-X. Liu, B.-X. Zhu, Z. Tao. Outer surface interactions to drive cucurbit[8]uril-based supramolecular frameworks: possible application in gold recovery. *Chem. Commun*, 2019, 55, 14271-14274.
- [25] F.-Y. Tian, R.-X. Cheng, Y.-Q. Zhang, Z. Tao, Q.-J. Zhu. Synthesis, Adsorption, and Recognition Properties of a Solid Symmetric Tetramethylcucurbit[6]uril-Based Porous Supramolecular Framework. *Aust. J. Chem*, vol. 2020, Article ID 9619461, 10 pages, 2020. <https://doi.org/10.1155/2020/9619461>
- [26] R.-X. Cheng, F.-Y. Tian, Y.-Q. Zhang, K. Chen, Q.-Jiang Zhu, Z. Tao. TMeQ[6]-based supramolecular frameworks assembled through outer surface interactions and their potential applications. *J. Mater. Sci.*, 2020, 55, 16497-16509.
- [27] M. Liu, M.-X. Yang, Y.-Q. Yao, Y.-J. Zhang, Y.-Q. Zhang, Z. Tao, Q.-J. Zhu, G. Wei, B. Bian, X. Xiao. Specific recognition of formaldehyde by a cucurbit[10]uril-based porous supramolecular assembly incorporating adsorbed 1, 8-diaminonaphthalene. *J. Mater. Chem. C*, 2019, 7, 1597-1603.
- [28] M. Liu, J.-L. Kan, Y.-Q. Yao, Y.-Q. Zhang, B. Bian, Z. Tao, Q.-J. Zhu, and X. Xiao. Facile preparation and application of luminescent cucurbit[10]uril-based porous supramolecular frameworks. *Sensors & Actuators: B. Chemical*, 2019, 283, 290–297.
- [29] H. Wu, J. Zhao, X.-N. Yang, D. Yang, L.-X. Chen, C. Redshaw, L.-G. Yang, Z. Tao, X. Xiao. A cucurbit[8]uril-based probe for the detection of the pesticide tricyclazole,

Dyes and Pigments, 2022, 199, 110076.

[30] C. Sun, Z.-Y. Wang, L.-D. Yue, Q.-X. Huang, Q. Cheng, R.-B. Wang. Supramolecular Induction of Mitochondrial Aggregation and Fusion. *J. Am. Chem. Soc.* 2020, 142, 16523-16527.

[31] S.-W. Guo, Q.-X. Huang, Y. Chen, J.-W. Wei, J. Zheng, L.-Y. Wang, Y.-T. Wang, R.-B. Wang. Synthesis and Bioactivity of Guanidinium-Functionalized Pillar[5]arene as a Biofilm Disruptor. *Angew. Chem. Int. Ed.* 2021, 60, 618-623.

[32] W.-B. Yang, A. Greenaway, X. Lin, R. Matsuda, A. J. Blake, C. Wilson, W. Lewis, P. Hubberstey, S. Kitagawa, N. R. Champness, M. Schröder. Exceptional thermal stability in a supramolecular organic framework: porosity and gas storage. *J. Am. Chem. Soc.* 2010, 132, 14457-14469.

[33] I. Hisaki, Y. Suzuki, E. Gomez, B. Cohen, N. Tohnai, A. Douhal. Docking strategy to construct thermostable, single-crystalline, hydrogen-bonded organic framework with high surface area. *Angew. Chem. Int. Ed.* 2018, 57: 12650-12655.

[34] G. Wittig, M. S. Über. Triphenyl-phosphin-methylene ALS olefinbildende Reagenzien I. *Chemische Berichte*, 1954, 87: 1318

[35] G. Wittig, H. W. Über. Triphenyl-phosphin-methylene ALS olefinbildende Reagenzien (II. Mitteil. 1)). *Chemische Berichte*, 1955, 88(11): 1654-1666

[36] A. Maercker. The Wittig reaction. *Organic Reaction*, 1965, 14: 270-490

[37] W. Carruthers. Some modern methods of organic synthesis. UK: Cambridge University Press, 1971, 77: 81-90

[38] K.-W. Kim, S.-H. Kwon, B.-J. Lee, S.-O. Ahn, J.-H. Lee, J.-H. Choi. Synthesis and photophysical properties of fluorescent dyes based on triphenylamine, diphenylamine, diphenyl sulfone or triphenyltriazine derivatives containing an acetylene linkage group. *Dyes and Pigments*, 2020, 181, 108617.

[39] S. Walker, R. Kaur, F. J. McInnes, N. J. Wheate. Synthesis, Processing and Solid State Excipient Interactions of Cucurbit[6]uril and Its Formulation into Tablets for Oral Drug Delivery. *Mol. Pharmaceutics*, 2010, 7, 6, 2166–2172.

[40] G. M. Sheldrick. *Acta Crystallogr. Sect. A*, 64, 112–122 (2008).

[41] G. M. Sheldrick, Crystal structure refinement with SHELXL, *Acta Cryst.* 2015,

C71, 3-8.

[42] O. V. Dolomanov, L. J. Bourhis, R. J. Gildea, J. A. K. Howard and H. Puschmann, OLEX2: A complete structure solution, refinement and analysis program, 2009. *J. Appl. Cryst.* 42, 339-341.

[43] A. Meng, J. Xing, Z.-J. Li, Q.-D. Li. Cr-Doped ZnO Nanoparticles: Synthesis, Characterization, Adsorption Property, and Recyclability. *ACS Appl. Mater. Interfaces*, 2015, 7, 49, 27449–27457

[44] R. Gong, J.-J. Ye, W. Dai, X.-Y. Yan, J. Hu, X. Hu, S. Li, H. Huang. Adsorptive Removal of Methyl Orange and Methylene Blue from Aqueous Solution with Finger-Citron-Residue-Based Activated Carbon. *Ind. Eng. Chem. Res.*, 2013, 52, 39, 14297–14303.